RSC Advances

PAPER

View Article Online
View Journal | View Issue

Cite this: *RSC Adv.*, 2023, **13**, 26275

Non-enzymatic amperometric glucose sensing on CuO/mesoporous TiO_2 modified glassy carbon electrode

Muhammad Ali,[a] Sadullah Mir[b] and Safeer Ahmed *[a]

The present study illustrates the fabrication of a glucose sensing electrode based upon binary composite of copper oxide and mesoporous titanium dioxide on glassy carbon (CuO/TiO_2/GCE). The X-ray diffraction, scanning electron microscopy and energy dispersive X-ray analysis evidently showed the phase pure monoclinic CuO nanoparticles and anatase TiO_2. N_2 adsorption–desorption analysis verified the mesoporosity in TiO_2 with specific surface area greater than 105 m^2 g^{-1}. Electrochemical impedance spectroscopic analysis proved the remarkable decrease in the charge transfer resistance and facilitation of electron transfer process on the fabricated electrode. The optimum weight ratio of CuO to TiO_2 was 1 : 1, and the optimum potential was 0.6 V *vs.* saturated calomel electrode. The chronoamperometric measurements displayed a detection limit of 1.9 μM, and sensitivities of 186.67 μA mM^{-1} cm^{-2} and 90.53 μA mM^{-1} cm^{-2} in two linear ranges of 0.05 to 5.2 mM and 5.2 to 20 mM, respectively. The amperometric analysis further showed good reproducibility, high specificity and outstanding stability of the modified electrode.

Received 17th July 2023
Accepted 28th August 2023

DOI: 10.1039/d3ra04787c

rsc.li/rsc-advances

1. Introduction

Glucose sensors have been developed for wide applications in different fields such as medical diagnosis, bioprocess monitoring, beverage industry, food industry, waste water treatment and fuel cells.[1,2] Diabetes mellitus is a disease marked by a high level of glucose (hyperglycemia) in the blood. Insufficient insulin production by the pancreas causes type 1 diabetes while type 2 can occur when the body cannot efficiently respond to the produced insulin. Insulin is the hormone that regulates blood glucose by signaling the body cells to take in glucose for energy or store it as glycogen when in excess.[3,4] Regular measurement of the blood sugar level is essential for the diagnosis of both types of diabetes. Type 1 diabetic patients may suffer from critical and chronic disorders, such as vision loss and limb amputation. Up to 90% of type 2 diabetics may develop cardiovascular disease, stroke, high blood pressure and renal failure.[5] Individuals with diabetes are prone to severe complications from COVID-19 infection.[6] Testing of the physiological glucose level is also crucial in order to prevent hypoglycemic situations that lead to blackouts and even death of the individual.[7,8]

The various methodologies that have been explored in the development of glucose sensors technology include electrochemical monitoring, optical (colorimetric) analysis, as well as piezoelectric and thermoelectric sensing.[3,9] Commercial glucose sensors have progressively developed from photometric to electrochemical enzymatic glucometers. The photometric devices demand the removal of interfering biomaterials such as red blood cells and rather large volumes of blood samples. Enzyme-based electrochemical biosensors have dominated the present-day glucose sensor industry.[10] This is because of certain advantages possessed by the enzymatic glucose sensors. These electrochemical biosensors have excellent selectivity to the target analyte and do not respond to the interfering agents.[11,12] These exhibit high sensitivity and hence low detection limit.[1,13,14] Furthermore, enzymatic tests give accurate and reliable results.[1,15] Despite having all these advantages the electrochemical enzymatic biosensors, however, suffer from shortcomings such as thermal and chemical instability, short service life, intricate enzyme immobilization processes and high-priced enzyme isolation and purification.[5,16,17] Because of these intrinsic flaws of enzymes, development of enzyme free glucose sensors has attracted significant research focus in recent years.[3,18]

Non-enzymatic sensors are regarded as the fourth-generation glucose sensors for analytical applications. Non-enzymatic glucose sensors are based on the electro-catalytic ability of noble metals such as Au,[19] Pt,[20] Pd,[21] Ag[22] *etc.*, transition metals like Cu,[23] Ni[24,25] *etc.*, their alloys (PtPb,[26] PtRu[2] *etc.*), metal sulfides (NiS),[27] oxides (Co_3O_4 [28,29] NiO,[25] CuO,[18,28] $NiCo_2O_4$,[30] Fe_3O_4 [31] *etc.*), carbon based nanostructured materials (carbon nanotubes,[32] doped diamond like materials,[33] graphene[34,35]) and conducting polymers.[36,37]

[a]*Department of Chemistry, Quaid-i-Azam University, 45320, Islamabad, Pakistan. E-mail: safeerad@qau.edu.pk; Fax: +92-51-90642241; Tel: +92-51-90642145*
[b]*Department of Chemistry, COMSATS University, Islamabad Campus, Pakistan*

Among these electrocatalysts, noble metals and their alloys have high electro-catalytic properties for glucose oxidation[28,38,39] However, high cost, relatively low selectivity, susceptibility to poisoning by various anions like Cl^- and HPO_4^{2-} [10,28]) and limited supply in nature[40] prevent their practical commercial applications. In contrast, a number of nanostructured earth abundant metals and their metal oxides catalysts for glucose electro-oxidization have been studied owing to their advantages such as; low cost, high stability, good sensitivity and rapid response.[1,41] The more earth abundant transition metals and metal oxides have reduced specific surface area because of their close packed structures and the metal oxides have poor electrical conductivity.[42] Therefore, carbon-based materials such as CNTs and graphene are mostly used to provide high surface area for loading metals or metal oxides nano-structured catalysts and for fast electron transfer between electrode and analyte.[40] However, because of their complicated and highly priced preparation methods, these are not fit for large scale applications. Various porous materials with high exposed surface area find their applications to enhance the analytical performance of non-enzymatic glucose sensors.[43] Based on pore diameter, nano porous solids are grouped into macroporous (having pore diameter > 50 nm), mesoporous (2–50 nm) and microporous (<2 nm) materials. Ordered mesoporous materials with regularly arranged mesopores of uniform size are prepared using structure-directing agents or templates. Soft-templating and hard-templating (nano casting) methods are used for the synthesis of these materials. Soft templating synthesis implies the use of surfactants or block copolymers as structure directing agents, whereas the later makes use of the already synthesized mesoporous solids like mesoporous silica (*e.g.*, MCM-41, SBA-15, KIT-6 *etc.*) or mesoporous carbon (CMK-3, CMK-1).[44–46]

Copper oxide (CuO) is one of the most extensively studied metal oxides because of its natural abundance, low cost associated with its production, good electrochemical and catalytic properties.[41] It is a p-type semiconductor with a narrow direct band gap of 1.2 eV and has found diverse applications in the fields of catalysis, photovoltaics, magnetic storage media, gas sensors, field-emission emitters, Li ion batteries and so on.[22,41,47] In comparison to pure elementary copper, CuO nanomaterials are more stable for electroanalysis.[23] CuO nanomaterials with a variety of morphologies and structures have been exploited for the fabrication of non-enzymatic glucose sensors, including nanoparticles,[48] nanowires,[49] nanorods,[50] mesoporous CuO[47] and nanosheets.[51] Various metals,[22,52] metal oxides[53–55] carbon nanomaterials[56,57] and conducting polymers have been incorporated to form CuO-based composite nanomaterials with improved sensitivity and specificity for the glucose.[36]

Titania (TiO_2) is another semiconductor and metal oxide which exists in different polymorphs and amorphous phases and is cost effective, chemically and thermally stable, environmentally friendly, biocompatible and possesses electronic and optical characteristics of the choice.[58] Due to these intrinsic features, TiO_2 has been applied in the areas ranging from photocatalysis, photovoltaics, biomedicine to sensors and photo/electrochromics.[59] A number of TiO_2-based nanocomposites have been explored for the enzyme free detection of glucose.[24,60,61] The existence of pores in the material mainly mesopores[62] increases the surface area and enhances the photocatalytic and physico-chemical properties such as adsorption, diffusion and access of chemical species to the reactive sites[58] which further extend its potential applications.[62–64] Mesoporous TiO_2 has been employed as gas sensor for H_2 and CO and displayed higher sensitivities than that fabricated with commercial TiO_2.[65,66]

As an alternative of carbon nanomaterials (carbon nanotubes and graphene), TiO_2 nanotube arrays with large surface area have been used as support material to load catalyst for the glucose sensing applications.[67] Pt nanoparticles decorated TiO_2 nano tube array (Pt/TiO_2 NTA),[67] TiO_2 nanotube arrays modified by CuO nanofibers (CuO/TiO_2)[55] and with Cu_2O nanoparticles [Cu_2O/TiO_2] electrodes have been used as non-enzymatic glucose sensors.[68] To the best of our knowledge, mesoporous TiO_2 based non-enzymatic glucose sensors have not been published so far. The present work employed CuO modified mesoporous TiO_2 dropped on glassy carbon electrode for the sensing of glucose, which was found to display better electrocatalytic activity with more sensitivity and stability towards glucose oxidation as compared to the previously reported TiO_2 nanotube based CuO/TiO_2 (ref. 55) and Cu_2O/TiO_2 modified electrodes.[68]

2. Experimental

2.1 Chemical reagents

Copper nitrate ($Cu(NO_3)_2$), ethylene glycol (99%) and ascorbic acid (AA) were purchased from Merk chemicals. Nafion (5% w/w) was obtained from Alfa Aesar. Titanium isopropoxide (97%), titanium chloride ($TiCl_4$) (Fluka ≥ 98%), cetyl trimethylammonium bromide (CTAB), D-glucose, lactose, maltose, D-fructose, D-galactose, uric acid (UA) and dopamine (DA) were obtained from Sigma-Aldrich and used as such. All the chemicals used were of analytical reagent grade purity and de-ionized water was used throughout the experiments.

2.2 Preparation of mesoporous titania

Mesoporous titania was prepared using mixed inorganic precursors, titanium isopropoxide and titanium chloride ($TiCl_4$) according to a reported method except the replacement of P123 by CTAB (Cetyl trimethylammonium bromide). In brief, 1 g of CTAB was dissolved in 20 g of ethyl alcohol under stirring. 0.6 g of $TiCl_4$ and 2.5 g of titanium isopropoxide were added to the solution and the mixture was kept stirring for further 2 hours. The mother solution was shifted to Petri-dishes for solvent evaporation and was gelled in an oven at 40 °C for 24 hours. Finally, the template was removed by calcination at 350 °C in air for 5 hours.[69]

2.3 Preparation of CuO

First 0.35 g $Cu(NO_3)_2$ was dissolved in 50 mL ethylene glycol solvent and the pH was adjusted 12.1 by the dropwise addition of 0.1 M NaOH. The solution was heated to 463 K for 3 h in an

oven. The acquired solution was filtered and dried to obtain the copper powder. The Cu powder so obtained was annealed in a furnace at 300 °C for half an hour in ambient conditions to form CuO nanoparticles.[34]

2.4 Material characterization

X-ray diffractometer (PANalytical X'PERT PRO diffractometer) with Cu Kα radiation source (λ = 0.1541 nm) was used to identify the phases of the synthesized materials. The morphology of the prepared samples was analyzed by Scanning electron microscope (JSM5910, JEOL Japan) equipped with energy dispersive X-ray spectroscopy (EDX) to detect the elemental composition of the samples. Surface area, pore size and pore volume of the prepared mesoporous titania nanoparticles were measured by N_2 adsorption/desorption isotherms using Quantachrome Nova 2200e instrument.

2.5 Electrochemical measurements

Electrochemical experiments like cyclic voltammetry (CV), electrochemical impedance spectroscopy (EIS) and chronoamperometry were performed with a Gamry instruments interface 1000E. A standard three electrode electrochemical cell was used with the modified glassy carbon electrode as the working electrode, saturated calomel electrode (Hg/Hg_2Cl_2) and a platinum wire as the reference and the counter electrodes, respectively.

2.6 Fabrication of modified electrode

1 mg each of CuO and TiO_2 samples were dispersed in a 1 mL mixture of de-ionized water and ethanol (1 : 1) and 10 μL of Nafion (5% w/w dispersion in water and 1-propanol) using sonication until ink type homogeneous black suspension was obtained. A glassy carbon electrode with surface area of 0.0707 cm^2 was polished with 0.3-micron alpha alumina powder followed by rinsing with de-ionized water as well as acetone and drying at room temperature. 10 μL of the ink was drop cast on the cleaned and polished surface of electrode and was then dried in an oven at 50 °C for half an hour to form the modified glassy carbon electrode represented as CuO/TiO_2/GCE. To optimize the composition of CuO and TiO_2, glassy carbon electrode was modified with different weight ratios of CuO and TiO_2.

3. Results and discussion

3.1 Characterizations of nanostructures

Fig. 1A presents the X-ray diffraction (XRD) pattern of the as synthesized CuO nanoparticles. The diffraction peaks observed at 2θ values of 31.75°, 35.28°, 38.37° and 48.56° correspond to the (110), (002), (111) and (−202) lattice planes, respectively. The appearance of these characteristic peaks indicates that CuO exhibits monoclinic structure (JCPDS no. 05-0661). Appearance of no other peak associated with the formation of any phase of impurities such as Cu, $Cu(OH)_2$ or Cu_2O was detected by XRD analysis, proving the high phase purity of CuO NPs. The average crystallite size of CuO nanoparticles calculated from Debye–Scherrer equation was found to be 12.7 nm.

Fig. 1B reveals the formation of anatase TiO_2. The peaks at 25.17°, 37.7°, 47.8°, 53.98°, 62.5°, 68.67° and 75° can be assigned to the (101), (103), (200), (105), (213), (116) and (107) crystal facets of anatase TiO_2 (JCPDS no. 01-0562). The average crystalline size was 14.034 nm.

Fig. 2A–C are the SEM images which show the morphologies of the synthesized CuO, TiO_2 and CuO/TiO_2, respectively. Mostly the particles of CuO (granular shape) in Fig. 2A reached the nanometer scale with an average size of 70 nm. Few CuO NPs appeared agglomerated which is the inherent property of CuO NPs.[70]

Fig. 2B presents the porous nanoparticles of TiO_2 which provide large surface area beneficial for the electrocatalytic activity of glucose, while 2C shows that CuO NPs are homogeneously distributed without obvious agglomeration and have not blocked completely the pores present in the TiO_2. The combination of CuO and TiO_2 produced the functionalized CuO/TiO_2 with large surface area which can increase the contact area and thus possibly the electrocatalytic activity of the modified electrode towards glucose.

The elemental composition of CuO/TiO_2 nanocomposite was studied by energy dispersive X-ray spectroscopy (EDS). The EDS spectrum in Fig. 2D indicates that the material obtained is composed of O, Ti and Cu elements. The Si peak

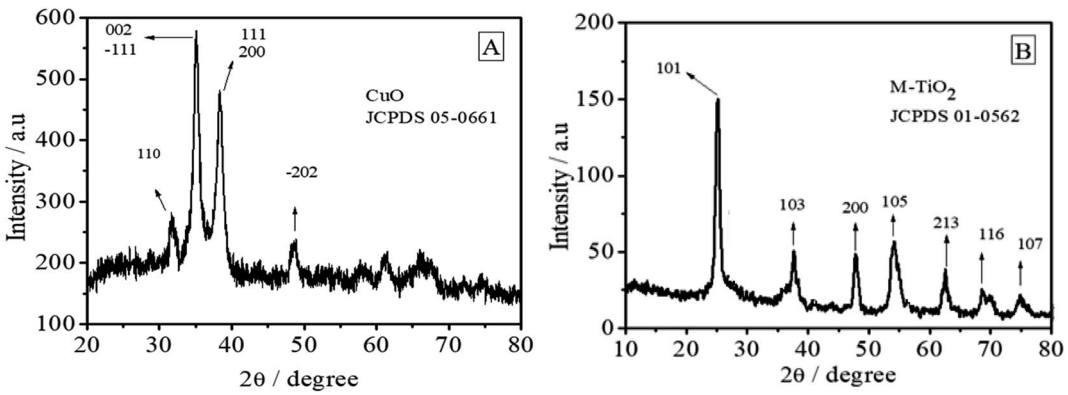

Fig. 1 XRD patterns of (A) the synthesized CuO nanoparticles and (B) mesoporous TiO_2.

originates from substrate. The obtained weight percentages of O, Ti and Cu are 29.51, 33.03 and 37.46%, respectively. The N_2 adsorption–desorption isotherm of M-TiO_2 at 77 K in Fig. 2E gives characteristic type IV isotherm, with H1 hysteresis loop implying the existence of mesopores in the material. An abrupt rise in adsorption volume associated with capillary condensation occurs at a high relative pressure P/P° of about 0.75. The prepared sample shows a specific surface area (S_{BET}) of 105.241 $m^2\ g^{-1}$ and pore volume of 0.324 $cm^3\ g^{-1}$. From the pore size distribution (Fig. 2F), TiO_2 has major pores centered at 7.795 nm along with minor pores at about 3 nm.

3.2 Electrochemical measurements

The electrochemical active surface area of a catalyst is an important performance indicator of an electrochemical sensor. Cyclic voltammetry (CV) was performed in standard redox solution of 5 mM $K_3Fe(CN)_6$ in 0.1 M KCl as supporting electrolyte at bare and modified electrode with a scan rate of 50 mV s^{-1}. Fig. 3A shows obvious enhancement in the reversible redox peak of the electron transfer of $[Fe(CN)]^{3-/4-}$ redox couple at CuO/TiO_2/GCE in comparison to bare electrode.

To estimate the effective surface areas of working electrodes, Randles–Sevcik equation of $I_P = 2.69 \times 10^5\ n^{3/2}AD^{1/2}\nu^{1/2}C$ was employed. Where I_p indicates the oxidation peak current (Amperes), n the number of electrons transferred in the half-reaction ($n = 1$), A the electroactive surface area (cm^2), D the diffusion coefficient (7.6×10^{-6} $cm^2\ s^{-1}$), ν the scan rate in V s^{-1} and C the probe concentration in mol cm^{-3}. The calculated areas of the bare GCE and CuO/TiO_2/GCE were 0.044 cm^2 and 0.0697 cm^2, respectively. Thus, the electroactive surface area of CuO/TiO_2 modified GCE enhanced considerably compared to bare electrode.

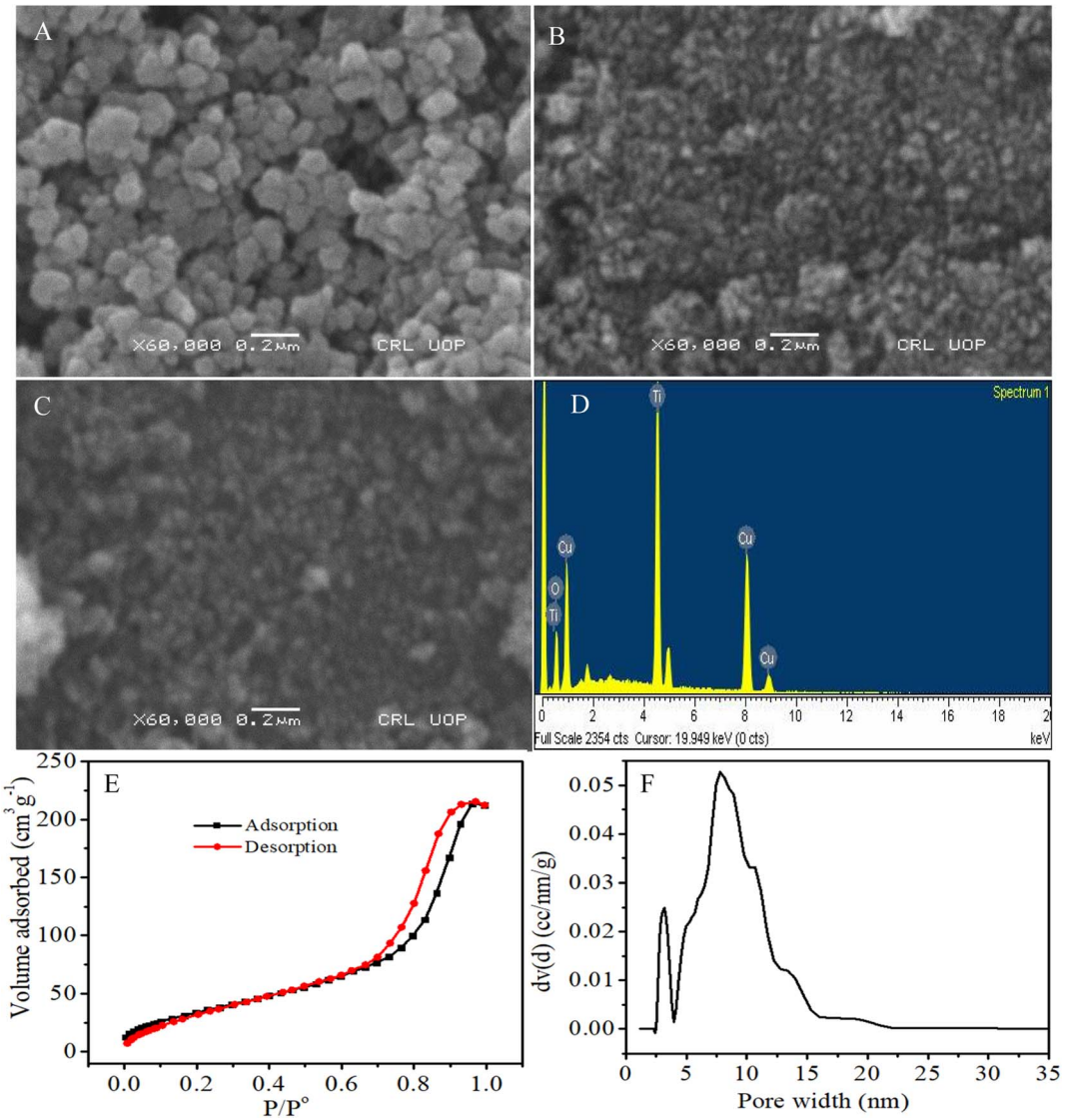

Fig. 2 (A) SEM image of the synthesized CuO NPs (B) TiO_2 templated by CTAB (C) CuO/TiO_2 (D) EDS spectrum of CuO/TiO_2 nanocomposite (E) nitrogen adsorption–desorption isotherm of M-TiO_2 and (F) pore size distribution of TiO_2.

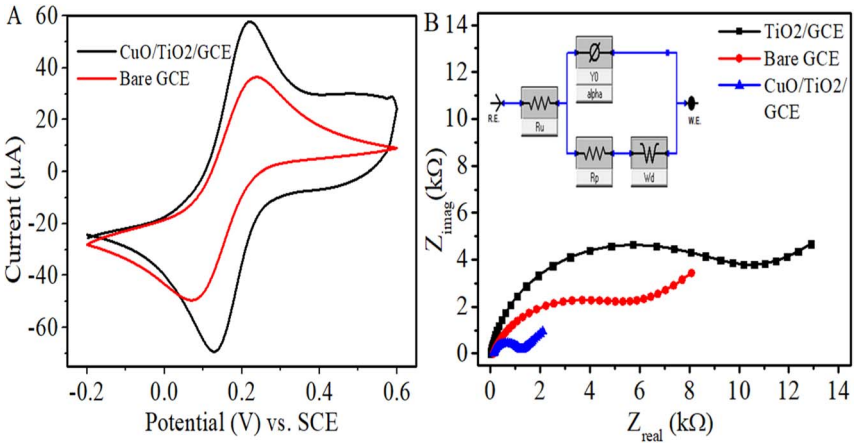

Fig. 3 (A) Cyclic voltammograms (A) and EIS Nyquist plots with applied frequency range from 100 kHz to 0.01 Hz, observed in 5 mM $K_3[Fe(CN)_6]$ in 0.1 M KCl at bare GCE and modified GCEs at 50 mV s^{-1} scan rate. Inset of (B) is the Randles equivalent circuit model for CuO/TiO_2/GCE.

In order to determine the charge transfer resistance at the electrode–electrolyte interface, the electrochemical impedance spectra (EIS) of bare GCE, TiO_2/GCE and CuO/TiO_2/GCE were observed in 0.1 M KCl having 5×10^{-3} M $K_3Fe(CN)_6$. The applied DC voltage was 0 V *vs.* OCP at 10 mV amplitude and AC frequency range applied of 0.1 Hz to 10^5 Hz as shown in Fig. 3B. Of the two portions of a typical Nyquist plot, the semicircle is at higher frequency range and the linear part is at smaller frequencies, concerning to the electron-transfer-limited and diffusion-limited processes, respectively. The diameter of the semicircle gives the electron-transfer resistance (R_{ct}) created at the electrode–electrolyte interface which assesses electrochemical performance of the system. From the Nyquist plots of various electrodes in the figure, the electron transfer resistance of TiO_2/GCE has been raised in comparison to that of bare GCE. This indicates that the semiconductor TiO_2 coating hampered the electron transfer between the redox probe and the surface of electrode. After the modification of electrode surface with CuO/TiO_2, the R_{ct} value decreased substantially even lower than that of bare GC surface, which suggests that CuO enhanced the electron transfer rate and improved the electrical conductivity of the as formed composite. Thus, for the purpose of enzyme free electrochemical detection of the glucose molecule, the CuO/TiO_2/GCE was chosen as an appropriate modified electrode. The EIS data were fitted by the Randles equivalent circuit model (inset of Fig. 3B) comprising of electrolyte resistance ($R_u = R_s$), charge transfer resistance ($R_p = R_{ct}$), capacitance (Y_0 = CPE) and Warburg impedance (W_d) elements. The values of various fitted electrochemical parameters acquired are given in Table 1.

The electrochemical oxidation of glucose was investigated in supporting electrolyte solution of 0.1 M NaOH at the surface of bare and modified GC electrodes using cyclic voltammetry. Fig. 4A depicts the cyclic voltammograms of bare glassy carbon, TiO_2, CuO and CuO/TiO_2 modified glassy carbon electrodes in the presence of 5 mM glucose in 0.1 M NaOH. From the figure, it is obvious that no redox peak of glucose is noticed for bare GCE and TiO_2/GCE or CuO/GCE. However, the CuO/TiO_2/GCE shows phenomenal sensitivity to glucose. This indicates the synergistic electrocatalysis between the CuO and TiO_2 which could be attributed to the relatively higher conductivity of CuO NPs and enhanced specific surface area of TiO_2 for sufficient loading of the CuO NPs in a uniformly dispersed manner.

Selection of optimum composition of CuO/TiO_2. Composition has a pronounced influence on the sensing ability of the electrochemical sensor. To get the right composition CuO was mixed with TiO_2 in different weight percentages such as 17, 29, 38, 45, 50, 55 and 60%. The samples were dispersed in a solution of water with ethanol (1 : 1) and 10 μL of Nafion using sonication to form the inks. Glassy carbon electrode was modified with the inks and cyclic voltammograms of the samples with different loads of CuO NPs were recorded in the presence of 5 mM glucose in 0.1 M NaOH. As observed from Fig. 4B, the anodic peak current associated with glucose oxidation goes on increasing with incrementing amount of loaded CuO NPs up to 50% and a further increase of the amount of loaded CuO NPs to 55 or 60 weight% adversely affected the sensing performance of the sensor. This suggests that 50% CuO loaded TiO_2 sample (CuO/TiO_2) shows the best electrocatalytic activity towards glucose oxidation.

Table 1 Electrochemical parameters of bare and modified GCEs from EIS analysis

Electrodes	R_{ct} (kΩ)	R_s (Ω)	CPE (nF)	W_d (10^{-6})	k_{app} (10^{-4} cm s^{-1})
Bare GCE	5.526	112.9	3092	115.3	2.19
TiO_2/GCE	9.616	11.7	417.5	45.01	—
CuO/TiO_2/GCE	1.038	118.9	818.4	594.1	7.36

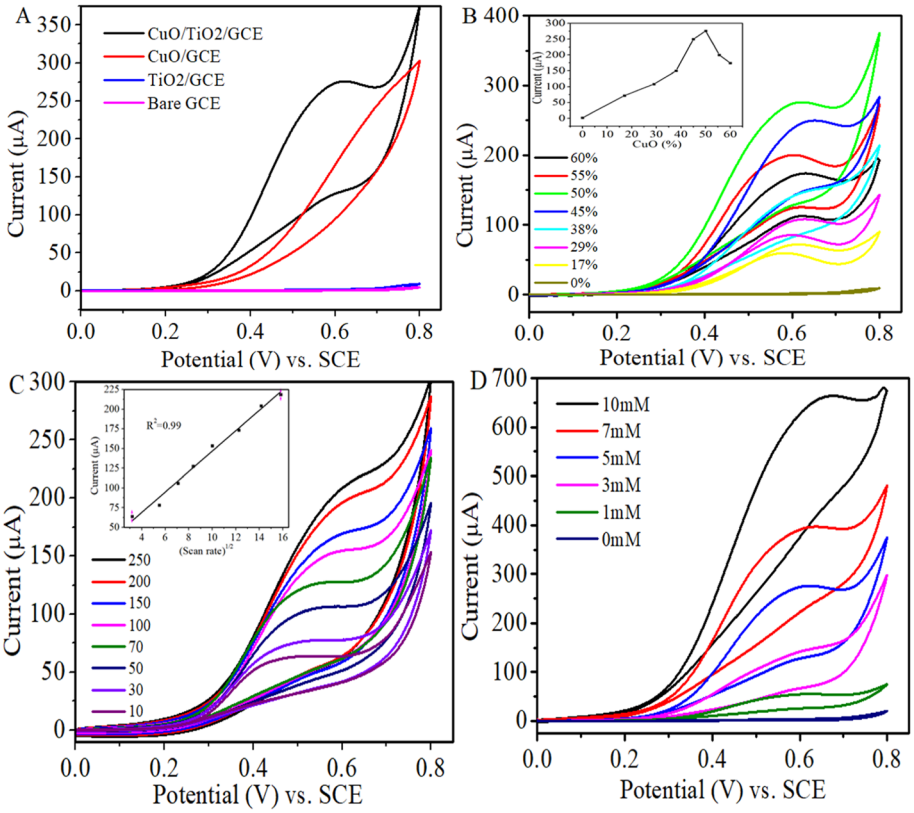

Fig. 4 (A) Cyclic voltammograms of 5 mM glucose in 0.1 M NaOH at bare and modified glassy carbon electrodes. Scan rate: 50 mV s^{-1}. (B) CVs of 5 mM glucose in 0.1 M NaOH at glassy carbon electrode modified with different weight percentages of CuO : TiO_2 composition. Scan rate: 50 mV s^{-1} (inset shows corresponding oxidation peak current of glucose as function of CuO load). (C) CVs of 3 mM glucose in 0.1 M NaOH at CuO/TiO_2/GCE performed under different scan rates (Inset is the plot of peak current to square root of scan rate). (D) CV responses of CuO/TiO_2/GCE in 0.1 M NaOH in the presence of various glucose concentrations. Scan rate: 50 mV s^{-1}.

The kinetics associated with the electro-oxidation of glucose at CuO/TiO_2/GCE as a function of scan rate was investigated in 0.1 M NaOH containing 3 mM glucose (Fig. 4C). It can be observed that an increase in the scan rate increased the oxidation peak current and the peak current is directly proportional to the square root of the scan rate, with a correlation co-efficient of 0.988 (inset: Fig. 4C). These results evidently indicate the diffusion-controlled fast electron transfer process. Moreover, the continuous shift in the peak potential with the increase in scan rate expresses the electrochemical irreversibility of the electron transfer process. The mesopores in the TiO_2 render channels for mass transport and increase the interfacial contact between the modified electrode and the electrolyte.

The electrochemical oxidation of glucose at CuO/TiO_2/GCE was also observed at different glucose concentrations in the range of 0 to 10 mM in 0.1 M NaOH (Fig. 4D). It is obvious that in the absence of glucose the voltammogram shows no redox peak, however, characteristic peak of glucose oxidation appears at around 0.6 V in the presence of glucose which proves the non-enzymatic sensitivity of CuO/TiO_2/GCE for glucose. The oxidation peak currents (i_{pa}) were enhanced with increasing glucose concentrations, nonetheless the peak position is slightly shifted to the more positive potential region. This could be due to the repulsive interaction experienced by the glucose molecules at high concentrations and their competition for the limited number of active sites on the electrode surface.[71]

3.3 Amperometric detection of glucose at CuO/TiO_2 modified glassy carbon electrode

The chronoamperometric response of CuO/TiO_2/GCE to glucose is illustrated in Fig. 5. To attain optimal amperometric response to the analyte glucose, the effect of varied applied potentials on the current response of CuO/TiO_2/GCE was analyzed. The corresponding amperometric responses of this modified electrode to the injection of 1 mM glucose into the continuously stirred 0.1 M NaOH at various applied potentials are given in Fig. 5A. The highest sensitivity value has been obtained at 0.6 V (*vs.* SCE). This observation correlates well with the cyclic voltammetry results and 0.6 V is taken as the optimum applied potential for the subsequent amperometric measurements.

Different glucose concentrations from 0.05 mM to 3 mM were successively added into 20 mL of the stirred 0.1 M NaOH after every 50 s at a constant applied potential of +0.6 V *vs.* SCE as shown in the Fig. 5B. After the injection of each aliquot of glucose, the modified electrode exhibited a quick stepwise increase in current response and the oxidation current acquired its steady state within 3 seconds indicating sufficiently fast kinetics of the electron transfer process and complementing the

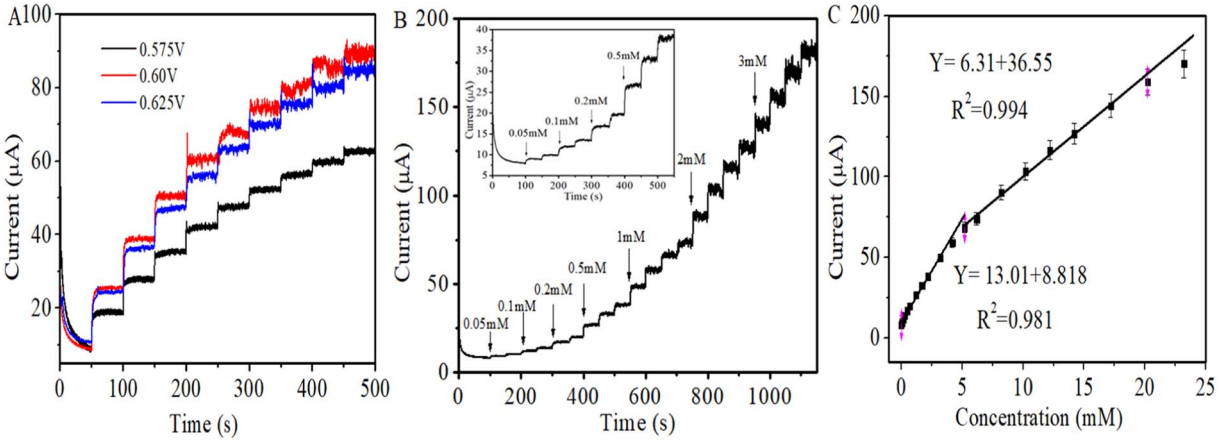

Fig. 5 Amperometric responses of CuO/TiO_2/GCE to the subsequent addition of (A) 1 mM glucose at different applied potentials (B) different glucose concentrations (0.05 to 3 mM) at 0.6 V into the continuously stirred 0.1 M NaOH solution. (C) The corresponding calibration curve.

CV results. Fig. 5C is the calibration curve for chronoamperometric current response of CuO/TiO_2/GCE towards glucose, which gives linear dependence between the oxidation current and the concentration of glucose in the range of 0.05 mM to 5.2 mM. The linear regression equation obtained is given by I_{pa} (μA) = 13.01X + 8.818, with correlation coefficient of $R^2 = 0.981$ ($N = 3$). The sensitivity of the sensor for glucose by employing this equation was calculated to be 186.67 μA mM^{-1} cm^{-2}, whereas detection limit was 1.9 μM (S/N = 3). The second linear range between the oxidation current and the glucose concentration was from 5.2 mM to 20 mM. The obtained linear regression equation is I_{pa} (μA) = 6.31X + 36.55, with a correlation coefficient of $R^2 = 0.994$ ($N = 3$). The sensitivity and detection limit were estimated to be 90.53 μA mM^{-1} cm^{-2} and 3.97 μM respectively.

The sensor exhibited wide linearity, however the lower sensitivity at higher concentration may be due to the adsorption of intermediates formed as a result of the electrocatalytic oxidation of glucose on the electrode surface which shields the active sites and obstructs the diffusion of glucose to the electrode surface.[35,72] The non-enzymatic glucose sensing performance of the fabricated sensor is compared with those of the already reported electrochemical sensors as shown in Table 2. The linear range, sensitivity and LOD of the fabricated sensor for glucose have been improved and in some cases the values are comparable with the recently reported work.

Reproducibility and stability. To examine the inter-electrode stability of CuO/TiO_2 modified GC electrode, five such electrodes were fabricated separately under the same conditions. Their sensitivity values to the sequential addition of 1 mM glucose to the electrochemical cell containing 0.1 M NaOH at 0.6 V were found as are shown in the Fig. 6A. The relative standard deviation (RSD) of these measurements was 5.89%, which indicates that the fabrication technique is precise, reliable, and fairly reproducible. Apart from reproducibility, another desirable feature of the CuO/TiO_2/GCE is the high-level operational stability. The current responses of one CuO/TiO_2 modified GC electrode to the introduction of 1 mM glucose for eight successive amperometric analyses are shown in the Fig. 6B. Where I_0 is the current response of the sensor to the analyte used for the first time and I is the current response after the subsequent runs. The amperometric response remained 88% of its initial value after 8th run and RSD was 8%, which reveals that the modified electrode is substantially stable and can be utilized repetitively (intra-electrode reproducibility). Likewise, the long-term stability of the sensor was tested by measuring its current response to 1 mM glucose solution under ambient conditions over four months. At the end of four

Table 2 Comparison of the performance of CuO/TiO_2/GCE with other non-enzymatic glucose sensors in 0.1 M NaOH medium with amperometry as detection method

Electrode	Sensitivity (μA mM^{-1} cm^{-2})	LOD (μM)	Linearity (mM)	Reference
Ni–Cu/TiO_2	719.9	30	0–6	24
CuO–Co_3O_4	1503.45	21.95	0–2	54
CuO/TiO_2/Ti	79.79	1	0–2	55
CuO/GO/GCE	262.52	0.69	0.00279–2.03	57
$Ni(OH)_2/TiO_2$	192	8	0.03–14	61
Pt/TiO_2 NTA	63.77	200	1–15	67
Cu_2O/TiO_2	14.56	62	3.0–9.0	68
Ti/TiO_2 NTA/Ni	200	4	0.1–1.7	73
CoNiCu	791, 322	0.5	0.05–1.55, 1.55–4.05	74
Au@CuO/LIG	1.124×10^6	1.8	0.005–5	75
CuO/TiO_2	186.67, 90.53	1.9	0.05–5.2, 5.2–20	This work

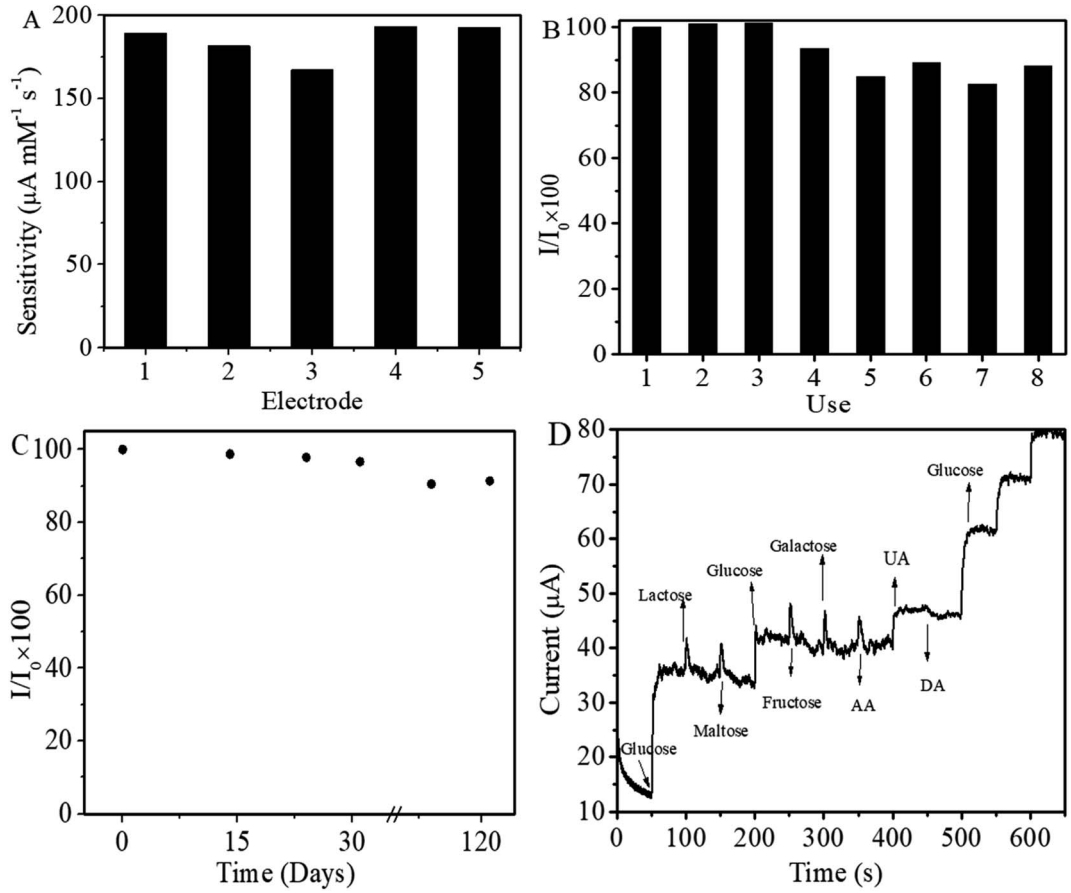

Fig. 6 (A) Comparison between the sensitivities of five CuO/TiO_2 modified GC electrodes. (B) Amperometric responses of one CuO/TiO_2/GCE to 1 mM glucose for eight times. (C) Long term stability of the sensor at ambient conditions for four months using 1 mM glucose in 0.1 M NaOH. (D) Amperometric response of CuO/TiO_2/GCE to 1 mM glucose and 0.1 mM of lactose, maltose, 0.3 mM of glucose, 0.1 mM of fructose, galactose, AA, UA, DA and 1 mM glucose.

months, the sensor retained 91% of its initial value (Fig. 6C). The highly stabile nature of the sensor electrode may be ascribed to the chemical stability of CuO[70] and to the mesoporosity of TiO_2 which besides raising the adsorption of glucose imparts support for the CuO NPs and suppressing their leaching or agglomeration. Thus, the modified glassy carbon electrode acts as a sensitive, reproducible, and durable non-enzymatic glucose sensor.

Anti-interfering ability/selectivity. Selectivity is an essential criterion for testing the analytical performance of non-enzymatic glucose sensors. The amperometric response of the sensor to various biomolecules such as lactose, maltose, fructose, galactose, AA, UA and dopamine *etc.*, which occur side by side with glucose in human blood was assessed. The concentration of these interfering compounds is about 30 to 50 times lower than that of glucose.[18] The anti-interference ability of the sensor was checked by adding 1 mM glucose to 0.1 M NaOH and then introducing different interferents at their physiological concentrations of 0.1 mM (ref. 76) with intervals as shown in the Fig. 6D. Compared to the oxidation current response of glucose, minor signals were observed for interfering agents, which indicates the selectivity of the sensor for the glucose oxidation at a fixed potential of 0.6 V. Since the concentrations of the glucose in human blood (3–8 mM) is much higher[76] with respect to interferents, the current responses of the interfering species are inferred to be insignificant during the practical sample analysis. The isoelectric point of CuO is 9.5, therefore the surface of CuO NPs would be negatively charged in NaOH solution. Interferents such as UA and AA, due to the loss of proton are also negatively charged in this solution and because of charge repulsion, the electrooxidation of these interferents is reduced and the selectivity is improved. Nafion film cation exchanger polymer on the interface may further contribute to the repelling effect and minimize the effect of these interferents.[77] Also, the oxidation of these interferents occurs at potentials other than the oxidation potential of glucose. Thus, the small amount of DA, AA, UA and other carbohydrate compounds will not affect the detection of glucose in blood and CuO/TiO_2 modified glassy carbon electrode is a reliable candidate for glucose detection in real samples.

4. Conclusion

The current study reports the development of non-enzymatic glucose sensor based on the CuO and mesoporous TiO_2 hybrid. The CuO/TiO_2 modified glassy carbon electrode

exhibited high electrocatalytic capability for glucose in basic medium. Based on electrochemical measurements, CuO/TiO_2/GCE displayed good analytical proficiency in the form of superior sensitivity, low detection limit (1.9 μM) and wide linearity range. The attainment can be attributed to the well-known activity of CuO and the enlarged surface area of mesoporous TiO_2. The modified electrode showed remarkable reproducibility, long term stability, high selectivity, and fast response. Our work implied that CuO/TiO_2 hybrid is a desirable material which manifests a great competence for the fabrication of high performance electrochemical non-enzymatic glucose sensor.

Data availability statement

The manuscript has no associated data.

Conflicts of interest

The authors declare that they have no conflict of interest.

Acknowledgements

Authors duly acknowledge Quaid-i-Azam University for the financial support through university research fund (URF). Thanks to Dr Shahid Bilal Butt (late) for useful discussions. The authors are also thankful to Muhammad Irfan from LUMS for the BET measurements. M. Ali is grateful to Higher Education Department KPK, Pakistan, for the grant of study leave for PhD studies at Quaid-i-Azam University Islamabad.

References

1 H. Zhu, L. Li, W. Zhou, Z. Shao and X. Chen, Advances in non-enzymatic glucose sensors based on metal oxides, *J. Mater. Chem. B*, 2016, **4**, 7333–7349.
2 K. E. Toghill and R. G. Compton, Electrochemical non-enzymatic glucose sensors: a perspective and an evaluation, *Int. J. Electrochem. Sci.*, 2010, **5**, 1246–1301.
3 K. Tian, M. Prestgard and A. Tiwari, A review of recent advances in nonenzymatic glucose sensors, *Mater. Sci. Eng. C.*, 2014, **41**, 100–118.
4 W. H. Organization, *World health statistics 2016: monitoring health for the SDGs sustainable development goals*, World Health Organization, 2016.
5 P. Si, Y. Huang, T. Wang and J. Ma, Nanomaterials for electrochemical non-enzymatic glucose biosensors, *RSC Adv.*, 2013, **3**, 3487–3502.
6 A. K. Singh, R. Gupta, A. Ghosh and A. Misra, Diabetes in COVID-19: prevalence, pathophysiology, prognosis and practical considerations, *Diabetes Metab. Syndr.*, 2020, **14**, 303–310, DOI: 10.1016/j.dsx.2020.04.004.
7 S. P. Nichols, A. Koh, W. L. Storm, J. H. Shin and M. H. Schoenfisch, Biocompatible materials for continuous glucose monitoring devices, *Chem. Rev.*, 2013, **113**, 2528–2549.
8 A. Heller and B. Feldman, Electrochemistry in diabetes management, *Acc. Chem. Res.*, 2010, **43**, 963–973.
9 N. R. Stradiotto, H. Yamanaka and M. V. B. Zanoni, Electrochemical sensors: a powerful tool in analytical chemistry, *J. Braz. Chem. Soc.*, 2003, **14**, 159–173, DOI: 10.1590/S0103-50532003000200003.
10 D.-W. Hwang, S. Lee, M. Seo and T. D. Chung, Recent advances in electrochemical non-enzymatic glucose sensors–a review, *Anal. Chim. Acta*, 2018, **1033**, 1–34.
11 C. Wei, X. Zou, Q. Liu, S. Li, C. Kang and W. Xiang, A highly sensitive non-enzymatic glucose sensor based on CuS nanosheets modified Cu_2O/CuO nanowire arrays, *Electrochim. Acta*, 2020, **334**, 135630.
12 S. Liu, W. Zeng and Y. Li, Synthesis of $ZnCo_2O_4$ microrods grown on nickel foam for non-enzymatic glucose sensing, *Mater. Lett.*, 2020, **259**, 126820.
13 C. Zhu, G. Yang, H. Li, D. Du and Y. Lin, Electrochemical sensors and biosensors based on nanomaterials and nanostructures, *Anal. Chem.*, 2015, **87**, 230–249.
14 F. Zhou, W. Jing, S. Liu, Q. Mao, Y. Xu, F. Han, Z. Wei and Z. Jiang, Electrodeposition of gold nanoparticles on ZnO nanorods for improved performance of enzymatic glucose sensors, *Mater. Sci. Semicond. Process.*, 2020, **105**, 104708.
15 Z. Zhu, L. Garcia-Gancedo, A. J. Flewitt, H. Xie, F. Moussy and W. I. Milne, A critical review of glucose biosensors based on carbon nanomaterials: carbon nanotubes and graphene, *Sensors*, 2012, **12**, 5996–6022.
16 J. Zhang, J. Ma, S. Zhang, W. Wang and Z. Chen, A highly sensitive nonenzymatic glucose sensor based on CuO nanoparticles decorated carbon spheres, *Sens. Actuators, B*, 2015, **211**, 385–391.
17 T.-W. Tsai, G. Heckert, L. F. Neves, Y. Tan, D.-Y. Kao, R. G. Harrison, D. E. Resasco and D. W. Schmidtke, Adsorption of glucose oxidase onto single-walled carbon nanotubes and its application in layer-by-layer biosensors, *Anal. Chem.*, 2009, **81**, 7917–7925.
18 S. K. Meher and G. R. Rao, Archetypal sandwich-structured CuO for high performance non-enzymatic sensing of glucose, *Nanoscale*, 2013, **5**, 2089–2099.
19 A. S. Shamsabadi, H. Tavanai, M. Ranjbar, A. Farnood and M. Bazarganipour, Electrochemical non-enzymatic sensing of glucose by gold nanoparticles incorporated graphene nanofibers, *Mater. Today Commun.*, 2020, **24**, 100963.
20 G. Wu, X. Song, Y.-F. Wu, X. Chen, F. Luo and X. Chen, Non-enzymatic electrochemical glucose sensor based on platinum nanoflowers supported on graphene oxide, *Talanta*, 2013, **105**, 379–385.
21 S. F. Bamsaoud, S. Rani, R. N. Karekar, S. Rani and S. W. Gosavi, Pd Doped SnO_2 Resistive Film As A Non-Enzymatic Glucose Sensor Glucose Sensor, *Hadhramout Univ. J. Inst. Nat. Appl. Sci.*, 2021, **14**, 169–178.
22 S. Felix, P. Kollu and A. N. Grace, Electrochemical performance of Ag–CuO nanocomposites towards glucose sensing, *Mater. Res. Innovations*, 2019, **23**, 27–32.
23 X. Kang, Z. Mai, X. Zou, P. Cai and J. Mo, A sensitive nonenzymatic glucose sensor in alkaline media with a copper nanocluster/multiwall carbon nanotube-modified glassy carbon electrode, *Anal. Biochem.*, 2007, **363**, 143–150.

24 A. Raziq, M. Tariq, R. Hussain, M. H. Mahmood, I. Ullah, J. Khan and M. Mohammad, Highly sensitive, non-enzymatic and precious metal-free electrochemical glucose sensor based on a Ni–Cu/TiO_2 modified glassy carbon electrode, *J. Serb. Chem. Soc.*, 2018, **83**, 733–744.

25 Q. Wang, S. Zheng, T. Li and Z. Wang, Ni/NiO multivalent system encapsulated in nitrogen-doped graphene realizing efficient activation for non-enzymatic glucose sensing, *Ceram. Int.*, 2021, **47**, 22869–22880, DOI: **10.1016/j.ceramint.2021.04.307**.

26 H.-F. Cui, J.-S. Ye, W.-D. Zhang, C.-M. Li, J. H. T. Luong and F.-S. Sheu, Selective and sensitive electrochemical detection of glucose in neutral solution using platinum–lead alloy nanoparticle/carbon nanotube nanocomposites, *Anal. Chim. Acta*, 2007, **594**, 175–183.

27 S. Luo, M. Yang, J. Li and Y. Wu, One-step potentiostatic electrodeposition of NiS-NiS_2 on sludge-based biochar and its application for a non-enzymatic glucose sensor, *RSC Adv.*, 2023, **13**, 5900–5907, DOI: **10.1039/d2ra07950j**.

28 S. Cheng, S. DelaCruz, C. Chen, Z. Tang, T. Shi, C. Carraro and R. Maboudian, Hierarchical Co_3O_4/CuO nanorod array supported on carbon cloth for highly sensitive non-enzymatic glucose biosensing, *Sens. Actuators, B*, 2019, **298**, 126860.

29 D. Ge, Y. Yang, X. Ni, J. Dong, Q. Qiu, X. Q. Chu and X. Chen, Self-template formation of porous Co_3O_4 hollow nanoprisms for non-enzymatic glucose sensing in human serum, *RSC Adv.*, 2020, **10**, 38369–38377, DOI: **10.1039/d0ra06453j**.

30 K. Naik Kusha, S. Kumar and C. S. Rout, Electrodeposited Spinel $NiCo_2O_4$ Nanosheet Arrays for Glucose Sensing Application, *RSC Adv.*, 2015, **5**, 74585–74591.

31 Z. Li, P. Huo, C. Gong, C. Deng and S. Pu, Boric-acid-modified Fe_3O_4@PDA @ UiO-66 for enrichment and detection of glucose by matrix-assisted laser desorption/ionization time-of-flight mass spectrometry, *Anal. Bioanal. Chem.*, 2020, **412**, 8083–8092.

32 R. Devasenathipathy, C. Karuppiah, S. M. Chen, S. Palanisamy, B. S. Lou, M. A. Ali and F. M. A. Al-Hemaid, A sensitive and selective enzyme-free amperometric glucose biosensor using a composite from multi-walled carbon nanotubes and cobalt phthalocyanine, *RSC Adv.*, 2015, **5**, 26762–26768, DOI: **10.1039/c4ra17161f**.

33 K. Zheng, H. Longn, Q. Wei, L. Ma, L. Qiao, C. Li, L. Meng, C.-T. Lin, Y. Jiang and T. Zhao, Non-enzymatic glucose sensor based on hierarchical Au/Ni/boron-doped diamond heterostructure electrode for improving performances, *J. Electrochem. Soc.*, 2019, **166**, B373.

34 Y.-W. Hsu, T.-K. Hsu, C.-L. Sun, Y.-T. Nien, N.-W. Pu and M.-D. Ger, Synthesis of CuO/graphene nanocomposites for nonenzymatic electrochemical glucose biosensor applications, *Electrochim. Acta*, 2012, **82**, 152–157.

35 J. Yang, Q. Lin, W. Yin, T. Jiang, D. Zhao and L. Jiang, A novel nonenzymatic glucose sensor based on functionalized PDDA-graphene/CuO nanocomposites, *Sens. Actuators, B*, 2017, **253**, 1087–1095.

36 A. Esmaeeli, A. Ghaffarinejad, A. Zahedi and O. Vahidi, Copper oxide-polyaniline nanofiber modified fluorine doped tin oxide (FTO) electrode as non-enzymatic glucose sensor, *Sens. Actuators, B*, 2018, **266**, 294–301.

37 Z. Li, W. Qian, H. Guo, X. Song, H. Yan, R. Jin and J. Zheng, Facile preparation of novel Pd nanowire networks on a polyaniline hydrogel for sensitive determination of glucose, *Anal. Bioanal. Chem.*, 2020, **412**, 6849–6858.

38 S. Park, S. Park, R.-A. Jeong, H. Boo, J. Park, H. C. Kim and T. D. Chung, Nonenzymatic continuous glucose monitoring in human whole blood using electrified nanoporous Pt, *Biosens. Bioelectron.*, 2012, **31**, 284–291.

39 S. Lee, J. Lee, S. Park, H. Boo, H. C. Kim and T. D. Chung, Disposable non-enzymatic blood glucose sensing strip based on nanoporous platinum particles, *Appl. Mater. Today.*, 2018, **10**, 24–29.

40 G. Chang, H. Shu, Q. Huang, M. Oyama, K. Ji, X. Liu and Y. He, Synthesis of highly dispersed Pt nanoclusters anchored graphene composites and their application for non-enzymatic glucose sensing, *Electrochim. Acta*, 2015, **157**, 149–157.

41 M. Rahman, A. J. Ahammad, J.-H. Jin, S. J. Ahn and J.-J. Lee, A comprehensive review of glucose biosensors based on nanostructured metal-oxides, *Sensors*, 2010, **10**, 4855–4886.

42 Y. Su, B. Luo and J. Z. Zhang, Controllable cobalt oxide/Au hierarchically nanostructured electrode for nonenzymatic glucose sensing, *Anal. Chem.*, 2016, **88**, 1617–1624.

43 X. Niu, X. Li, J. Pan, Y. He, F. Qiu and Y. Yan, Recent advances in non-enzymatic electrochemical glucose sensors based on non-precious transition metal materials: opportunities and challenges, *RSC Adv.*, 2016, **6**, 84893–84905.

44 B. Szczęśniak, J. Choma and M. Jaroniec, Major advances in the development of ordered mesoporous materials, *Chem. Commun.*, 2020, **56**, 7836–7848, DOI: **10.1039/d0cc02840a**.

45 S. Savic, K. Vojisavljevic, M. Počuča-Nešić, K. Zivojevic, M. Mladenovic and N. Knezevic, Hard Template Synthesis of Nanomaterials Based on Mesoporous Silica, *Metall. Mater. Eng.*, 2018, **24**, 225–241, DOI: **10.30544/400**.

46 S. Jun, S. H. Joo, R. R. Yoo, M. Kruk, M. Jaroniec, Z. Liu, T. Ohsuna and O. Terasaki, Synthesis of new, nanoporous carbon with hexagonally ordered mesostructure, *J. Am. Chem. Soc.*, 2000, **122**, 10712–10713, DOI: **10.1021/ja002261e**.

47 S. Liu, Z. Wang, F. Wang, B. Yu and T. Zhang, High surface area mesoporous CuO: a high-performance electrocatalyst for non-enzymatic glucose biosensing, *RSC Adv.*, 2014, **4**, 33327–33331.

48 S. Liu, J. Tian, L. Wang, X. Qin, Y. Zhang, Y. Luo, A. M. Asiri, A. O. Al-Youbi and X. Sun, A simple route for preparation of highly stable CuO nanoparticles for nonenzymatic glucose detection, *Catal. Sci. Technol.*, 2012, **2**, 813–817.

49 Z. Zhao, Q. Li, Y. Sun, C. Zhao, Z. Guo, W. Gong, J. Hu and Y. Chen, Highly sensitive and portable electrochemical detection system based on AuNPs@CuO NWs/Cu_2O/CF hierarchical nanostructures for enzymeless glucose sensing, *Sens. Actuators, B*, 2021, **345**, 130379, DOI: **10.1016/j.snb.2021.130379**.

50 D. Wang, C. Zheng, Y. Li, C. Han, H. Fang, X. Fang and H. Zhao, Sensitive non-invasive electrochemical sensing of glucose in saliva using amorphous SnO_x decorated one-dimensional CuO nanorods rich in oxygen vacancy defects, *Appl. Surf. Sci.*, 2022, **592**, 153349, DOI: 10.1016/j.apsusc.2022.153349.

51 J. Lv, C. Kong, Y. Xu, Z. Yang, X. Zhang, S. Yang, G. Meng, J. Bi, J. Li and S. Yang, Facile synthesis of novel CuO/Cu_2O nanosheets on copper foil for high sensitive nonenzymatic glucose biosensor, *Sens. Actuators, B*, 2017, **248**, 630–638.

52 B. Zheng, G. Liu, A. Yao, Y. Xiao, J. Du, Y. Guo, D. Xiao, Q. Hu and M. M. F. Choi, A sensitive AgNPs/CuO nanofibers non-enzymatic glucose sensor based on electrospinning technology, *Sens. Actuators, B*, 2014, **195**, 431–438.

53 T. Dayakar, K. V. Rao, K. Bikshalu, V. Malapati and K. K. Sadasivuni, Non-enzymatic sensing of glucose using screen-printed electrode modified with novel synthesized CeO_2@CuO core shell nanostructure, *Biosens. Bioelectron.*, 2018, **111**, 166–173.

54 D. Wang, H. M. Zhao, L. Guo, L. Zhang, H. Bin Zhao, X. Fang, S. Li and G. Wang, Facile synthesis of CuO–Co_3O_4 prickly-sphere-like composite for non-enzymatic glucose sensors, *Rare Met.*, 2022, **41**, 1911–1920, DOI: 10.1007/s12598-021-01939-2.

55 S. Luo, F. Su, C. Liu, J. Li, R. Liu, Y. Xiao, Y. Li, X. Liu and Q. Cai, A new method for fabricating a CuO/TiO_2 nanotube arrays electrode and its application as a sensitive nonenzymatic glucose sensor, *Talanta*, 2011, **86**, 157–163.

56 L.-C. Jiang and W.-D. Zhang, A highly sensitive nonenzymatic glucose sensor based on CuO nanoparticles-modified carbon nanotube electrode, *Biosens. Bioelectron.*, 2010, **25**, 1402–1407.

57 J. Song, L. Xu, C. Zhou, R. Xing, Q. Dai, D. Liu and H. Song, Synthesis of graphene oxide based CuO nanoparticles composite electrode for highly enhanced nonenzymatic glucose detection, *ACS Appl. Mater. Interfaces*, 2013, **5**, 12928–12934.

58 B. Bonelli, S. Esposito and F. S. Freyria, Mesoporous Titania: Synthesis, Properties and Comparison with Non-Porous Titania, in *Titan. Dioxide*, InTech, 2017, DOI: DOI: 10.5772/intechopen.68884.

59 X. Chen and S. S. Mao, Titanium dioxide nanomaterials: synthesis, properties, modifications, and applications, *Chem. Rev.*, 2007, **107**, 2891–2959.

60 A. Al-Mokaram, M. A. A. Amir, R. Yahya, M. M. Abdi and H. N. M. E. Mahmud, The development of non-enzymatic glucose biosensors based on electrochemically prepared polypyrrole–chitosan–titanium dioxide nanocomposite films, *Nanomaterials*, 2017, **7**, 129.

61 A. Gao, X. Zhang, X. Peng, H. Wu, L. Bai, W. Jin, G. Wu, R. Hang and P. K. Chu, *In situ* synthesis of Ni$(OH)_2$/TiO_2 composite film on NiTi alloy for non-enzymatic glucose sensing, *Sens. Actuators, B*, 2016, **232**, 150–157.

62 R. Zhang, A. A. Elzatahry, S. S. Al-deyab and D. Zhao, Mesoporous titania: from synthesis to application, *Nano Today*, 2012, **7**, 344–366, DOI: 10.1016/j.nantod.2012.06.012.

63 W. Li, Z. Wu, J. Wang, A. A. Elzatahry and D. Zhao, A perspective on mesoporous TiO_2 materials, *Chem. Mater.*, 2014, **26**, 287–298.

64 G. J. de A. A. Soler-Illia, A. Louis and C. Sanchez, Synthesis and characterization of mesostructured titania-based materials through evaporation-induced self-assembly, *Chem. Mater.*, 2002, **14**, 750–759.

65 G. S. Devi, T. Hyodo, Y. Shimizu and M. Egashira, Synthesis of mesoporous TiO_2-based powders and their gas-sensing properties, *Sens. Actuators, B*, 2002, **87**, 122–129.

66 J. Ma, Y. Li, J. Li, X. Yang, Y. Ren, A. A. Alghamdi, G. Song, K. Yuan and Y. Deng, Rationally Designed Dual-Mesoporous Transition Metal Oxides/Noble Metal Nanocomposites for Fabrication of Gas Sensors in Real-Time Detection of 3-Hydroxy-2-Butanone Biomarker, *Adv. Funct. Mater.*, 2022, **32**, 1–13, DOI: 10.1002/adfm.202107439.

67 Y. Wang, J. Chen, C. Zhou, L. Zhou, Y. Kong, H. Long and S. Zhong, A novel self-cleaning, non-enzymatic glucose sensor working under a very low applied potential based on a Pt nanoparticle-decorated TiO_2 nanotube array electrode, *Electrochim. Acta*, 2014, **115**, 269–276.

68 M. Long, L. Tan, H. Liu, Z. He and A. Tang, Novel helical TiO_2 nanotube arrays modified by Cu_2O for enzyme-free glucose oxidation, *Biosens. Bioelectron.*, 2014, **59**, 243–250.

69 B. Tian, H. Yang, X. Liu, S. Xie, C. Yu, J. Fan, B. Tu and D. Zhao, Fast preparation of highly ordered nonsiliceous mesoporous materials *via* mixed inorganic precursors, *Chem. Commun.*, 2002, 1824–1825.

70 W. Zheng, L. Hu, L. Y. S. Lee and K.-Y. Wong, Copper nanoparticles/polyaniline/graphene composite as a highly sensitive electrochemical glucose sensor, *J. Electroanal. Chem.*, 2016, **781**, 155–160.

71 W. Zhang, G. Jia, H. Li, S. Liu, C. Yuan, Y. Bai and D. Fu, Morphology-Modulated Mesoporous CuO Electrodes for Efficient Interfacial Contact in Nonenzymatic Glucose Sensors and High-Performance Supercapacitors, *J. Electrochem. Soc.*, 2016, **164**, B40–B47.

72 X. Wang, E. Liu and X. Zhang, Non-enzymatic glucose biosensor based on copper oxide-reduced graphene oxide nanocomposites synthesized from water-isopropanol solution, *Electrochim. Acta*, 2014, **130**, 253–260.

73 C. Wang, L. Yin, L. Zhang and R. Gao, Ti/TiO_2 nanotube array/Ni composite electrodes for nonenzymatic amperometric glucose sensing, *J. Phys. Chem. C*, 2010, **114**, 4408–4413.

74 K. Ghanbari and Z. Babaei, Fabrication and characterization of non-enzymatic glucose sensor based on ternary NiO/CuO/polyaniline nanocomposite, *Anal. Biochem.*, 2016, **498**, 37–46.

75 F. Cui, H. Sun, X. Yang, H. Zhou, Y. Wu, J. Li, H. Li, J. Liu, C. Zeng, B. Qu, J. Zhang and Q. Zhou, Laser-induced graphene (LIG)-based Au@CuO/V_2CT_x MXene non-enzymatic electrochemical sensors for the urine glucose test, *Chem. Eng. J.*, 2023, **457**, 141303, DOI: 10.1016/j.cej.2023.141303.

76 Z. Yang, X. Zheng and J. Zheng, A facile one-step synthesis of Fe_2O_3/nitrogen-doped reduced graphene oxide

nanocomposite for enhanced electrochemical determination of dopamine, *J. Alloys Compd.*, 2017, **709**, 581–587.

77 X. Gong, Y. Gu, F. Zhang, Z. Liu, Y. Li, G. Chen and B. Wang, High-performance non-enzymatic glucose sensors based on CoNiCu alloy nanotubes arrays prepared by electrodeposition, *Front. Mater.*, 2019, **6**, 3.